



THERMAL ANALYSIS OF MEMS-BASED
THERMOELECTRICALLY CONTROLLED
MICRONOZZLE

BY

AMAR HASAN HAMEED

A thesis submitted in fulfillment of the requirement
for the degree of Doctor of Philosophy

Kulliyyah of Engineering
International Islamic University
Malaysia

JANUARY 2012

ABSTRACT

A new technique which implements heating upstream of the micronozzle throat and cooling downstream of the throat through the side-walls of the micronozzle is proposed. Thermoelements are used to pump heat from the cold section (supersonic) to the hot section (subsonic) of the micronozzle using Peltier effect. The proposed micronozzle is given herein the name Thermo-electrically Controlled Micronozzle (TECMN). A generalized quasi-one-dimensional model is developed to solve the flow of gaseous propellant inside the micronozzle in the presence of heat pumping from the supersonic to the subsonic through the side walls. The improvement in the efficiency due to using TECMN is verified, which is more significant for reduced divergent wall temperature and mass flow rate. The model also involves the thermoelectricity effects in the solid walls. A general energy equation of one-dimensional heat transfer in a non-uniform wall subjected to a longitudinal electrical field and lateral heat convection is developed and solved analytically for uniform wall and numerically for non-uniform walls. A set of non-dimensional parameters which affects the performance of the TECMN are identified and studied for better heat exchange with the flowing gas. It is found that the uniform TE wall performs better than non-uniform wall in heating-cooling process. The two-dimensional laminar Navier-Stokes equations are solved numerically for gas flow in a micronozzle for different thermal boundary conditions; isothermal divergent wall, uniform heating, and non-uniform heating-cooling in uniform side-walls. The non-uniform heating-cooling boundary condition is a imitation of the thermoelectric wall. It is found that heating upstream the throat always affect mass flow rate, while heating downstream the throat increases the thrust which may decrease with any mass flow reduction, however the thrust per unit mass flow and viscous losses increase always with heating. It is found that heat supply in the convergent-divergent side-wall results in enhancement of thrust level, specific impulse, mass consumption saving, and efficiency of specific impulse. Outcome of heat developing to/absorbing from a gas flowing into a convergent-divergent micronozzle for a range of Reynolds numbers below 10^3 is investigated assuming one-dimensional thermal analysis of a uniform side-wall. It was found that the improvement in the specific impulse efficiency increases with decreasing Reynolds number. This improvement reaches up to 9.35% at $Re = 15$ during the heating-cooling process through the side-walls. Heating process and heating-cooling process through the wall are more useful to improve efficiency at low Reynolds numbers below 100. This research concludes that the utilization of thermoelectricity to supply heat upstream of micronozzle throat and remove heat downstream of throat through thermoelement side walls is very useful to improve the micronozzle efficiency and reduces propellant consumption.

خلاصة البحث

المنافث الدقيقة تعاني من خسائر لزوجة الغاز وخاصة عند ارقام Reynolds المنخفضة. بعد عمل استقصاء ودراسة انظمة الدفع الميكانيكية المستخدمة، تم اقتراح تقنية جديدة وهي المنافث المتحكم به الكترودحراريا (TECMN) لغرض الحصول على منافث ذي اداء افضل. مبدأ عمل هذه التقنية هو القيام بتسخين الجدار الجانبي قبل الخانق والتبريد للجدار بعد الخانق لغرض تسخين الغاز ثم تبريده من خلال الجدار حيث يعتقد انه سيحسن من كفاءة واداء المنافث. تسخين و تبريد طرفي الجدار سيكون بواسطة تصنيع الجدار من قطعة الكترودحرارية تعمل حسب مبدأ Peltier. تم حل المعادلة العامة شبيهة احادية الاتجاه عدديا في نموذج لمنفث دقيق مع تسخين الغاز الذي يجري بسرعة تحت السرعة الصوتية وتبريده عندما يكون بسرعة تفوق السرعة الصوتية ووجد تحسن في اداء المنافث. اما الجدار اللالكترودحراري لهذه التقنية فقد تمت دراسته ايضا بصورة مفصلة. فقد تمت كتابة المعادلة التفاضلية لنموذج للجدار ذو شكل غير منتظم المقطع وباعتبار كل الاحمال الحرارية و الكهربائية ومن ضمنها انتقال الحرارة العالي على جانب الجدار. وكذلك تم حل النموذج عدديا وتم حل نموذج منتظم المقطع تحليليا لغرض المقارنة. وتم دراسة النماذج بوجود تغيرات في عوامل رئيسية محسوبة بدون وحدات قياس لغرض معرفة تأثير هذه العوامل على اداء هذه التقنية. لقد تم حل معادلة الجريان الثنائي الابعاد و الخاضعة لقوانين حفظ المادة والطاقة في المنافث الدقيقة عدديا و تحت عدة ظروف حدودية على جدار المنافث و هي: جدار الجزء المنفرج ذو دراجة الحرارة الثابتة، و توليد حرارة منتظم داخل جدار المنافث، وتوليد وامتصاص الحرارة بشكل غير منتظم داخل جدار المنافث. وقد اظهرت النتائج عند توليد الحرارة المنتظم تحسنا ملحوظا في قيمة الدفع والاندفاع النوعي و تقليل جريان الغاز وكذلك تحسين كفاءة الاندفاع النوعي للمنفث. عند ظروف توليد وامتصاص الحرارة بشكل غير منتظم في الجدار تم عمل الاختبار ضمن مدى ارقام رينولدز (Re) اقل من 10^3 وكذلك تم حل معادلات الغاز احادية البعد للتنبؤ بانتقال الحرارة داخل الجدار ذي المقطع المنتظم. لقد وجد ان التحسن في كفاءة الاندفاع النوعي للمنفث تتزايد بشكل ملحوظ عند ارقام رينولدز تتراوح عند 100 او اقل، و قد وصل التحسن بزيادة قدرها 9.35% عند رقم رينولدز (Re=15) اثناء عملية تسخين و تبريد جدار المنافث. بالاضافة الى انه عملية التبريد و التسخين المزدوج تعطي نتائج افضل من التسخين المنتظم في تقليل والاقتصاد جريان الغاز في المنافث.

APPROVAL PAGE

The Thesis of Amar Hasan Hameed has been approved by the following:

Raed Ismail Kafafy
Supervisor

Waqar Asrar
Co-Supervisor

Moumen Mohammed Idres
Co-Supervisor

Ashraf Ali Omar
Internal Examiner

M. N. A. Hawlader
Internal Examiner

Mohammad Nazri Mohd Jaafar
External Examiner

Radwan Jamal Elatrash
Chairman

DECLARATION

I hereby declare that this thesis is the result of my own investigations, except were otherwise stated. I also declare that it has not been previously and concurrently submitted as a whole for any other degrees at IIUM or other institutions.

Amar Hasan Hameed

Signature.....

Date.....

INTERNATIONAL ISLAMIC UNIVERSITY MALAYSIA

**DECLARATION OF COPYRIGHT AND AFFIRMATION
OF FAIR USE OF UNPUBLISHED RESEARCH**

Copyright © 2011 by International Islamic University Malaysia. All Rights Reserved.

**THERMAL ANALYSIS OF MEMS-BASED THERMOELECTRICALLY
CONTROLLED MICRONOZZLE**

I hereby affirm that The International Islamic University Malaysia (IIUM) holds all rights in the copyright of this work and henceforth any reproduction or use in any form or by means whatsoever is prohibited without the written consent of IIUM. No part of this unpublished research may be reproduced, stored in a retrieval system, or transmitted, in any form or by means, electronic, mechanical, photocopying, recording or otherwise without prior written permission of the copyright holder.

Affirmed by Amar Hasan Hameed

.....
Signature

.....
Date

ACKNOWLEDGEMENTS

In the Name of Allah, the Most Compassionate, the Most Merciful. All praise and thanks should be to ALLAH (S.W.T.) the Almighty, who enabled me to live and accomplish this work. Prayers and peace be upon the messenger of Allah, Prophet Mohammed (P.B.U.H.).

First, I would like to express my sincere appreciation and gratitude to my supervisors; Dr. Raed Kafafy, Prof. Dr. Waqar Asrar and Dr. Moumen Idres, for their excellent supervision, guidance, encouragement and support. I am also grateful to them for providing the opportunities to publish this work, both in journals and at conferences.

I would like to express heartfelt gratitude to my parents who have never given up praying for my success from very beginning of my life. Without them, I would not be the person I am today. My deep and sincere gratitude goes to my beloved wife, my sons and my daughters whose continuous motivation, affection, and moral support have enabled me to complete this work. I would like to dedicate this work to my parents, my brothers, my sisters and my family.

I would like to express my sincere thanks to my colleagues and friends in ECTMRG post-graduate room, Omer, Abdulhafid, Amri, Al-turki, Nabeel, Eshrif and AbdulKhaliq, for their friendly cooperation and support.

Lastly, I offer my regards and blessings to all of those who supported me in any respect during the completion of the project.

TABLE OF CONTENTS

Abstract	ii
Arabic abstract.....	iii
Approval Page.....	iv
Declaration Page.....	v
Copyright Page.....	vi
Acknowledgment.....	vii
List of Tables.....	x
List of Figures.....	xi
List of Symbols	xv
List of Abbreviations	xix
CHAPTER 1: INTRODUCTION.....	1
1.1 Background.....	1
1.2 Thermoelectrically Controlled Micronozzle.....	2
1.3 Thermoelectricity.....	4
1.4 Problem Statement and Its Significance	7
1.5 Research Philosophy.....	8
1.6 Research Objectives.....	9
1.7 Research Methodology	9
1.8 Scope of Research.....	13
1.9 Thesis Organization	13
CHAPTER 2: LITERATURE REVIEW.....	15
2.1 Introduction	15
2.2 MEMS-Based Micropropulsion Systems	16
2.3 One-Dimensional Analysis.....	19
2.3.1 Gas Flow.....	19
2.3.2 Heat Transfer in Thermoelements.....	21
2.4 Two-Dimensional Flow	25
2.5 Summary.....	33
CHAPTER 3: THIORETICAL ASSESSMENT AND METHODOLOGY	35
3.1 Introduction.....	35
3.2 Micropropulsion System.....	36
3.3 One-Dimensional Flow.....	38
3.3.1 Thermal Efficiency.....	41
3.3.2 Thermodynamics of Micronozzle	44
3.3.3 Heat Transfer of Micronozzle	45
3.4 Thermoelement as a Side Wall	46
3.4.1 Uniform TE Wall.....	47
3.4.2 Non-Uniform TE Wall	52
3.5 Two-Dimensional Flow	58
3.5.1 Micronozzle Model	60

3.5.2	Governing Equations and Boundary Conditions.....	62
3.5.3	Micronozzle Performance	69
3.6	Summary	70
CHAPTER 4:	ONE-DIMENSIONAL OF GAS FLOW AND THERMOELEMENT.....	71
4.1	Introduction.....	71
4.2	Quasi-One-Dimensional Flow	73
4.2.1	Combination of Two Influences.....	73
4.2.2	Thermal Efficiency.....	76
4.2.3	Cooling Parameters	79
4.3	Quasi-One-Dimensional Analysis of Thermoelectric Wall.....	82
4.3.1	Non-Uniform TE Wall	82
4.3.2	Uniform TE Wall.....	90
4.4	Summary	93
CHAPTER 5:	TWO DIMENSIONAL FLOW IN A MICRONOZZLE.....	95
5.1	Introduction.....	95
5.2	Grid-Independence Study	97
5.3	Isothermal Divergent Wall.....	99
5.3.1	Mach Contours	99
5.3.2	Profiles at Micronozzle Exit.....	101
5.4	Heated Side-Wall.....	108
5.5	Thermoelectric Side-Wall.....	122
5.6	Summary	131
CHAPTER 6:	CONCLUSION AND RECOMMENDATION.....	133
6.1	Conclusion	133
6.2	Research Contribution	135
6.3	Recommendations for Future Work.....	136
BIBILOGHRAPHY	138	
APPENDIX I:	FLOW CHART OF 1D FLOW.....	144
APPENDIX I:	RUNGE-KUTTA SCHEME.....	145

LIST OF TABLES

<u>Table No.</u> <u>No.</u>		<u>Page</u>
4.1	Performance elements of a micronozzle for several cases of wall heating and cooling, $Kn=0.00048$.	78
5.1	Cases nomination and description	110
5.2	Mass flow rate and thrust variations with cases of specified stagnation pressure.	113
5.3	Stagnation pressure and thrust variations with the cases for specified mass flow rate.	115
5.4	Extended wall geometry results for specified mass flow rate and constant viscosity.	116
5.5	Extended wall geometry results for specified stagnation pressure and constant viscosity, $Re=40$.	122
5.6	Nominal melting temperature for high temperature fixed points (HTFPs)	127
5.7	Stagnation pressure drop and kinetic energy per unit mass production for constant and variable viscosity for several input power and $Re=40$.	130

LIST OF FIGURES

<u>Figure No.</u>	<u>Page No.</u>
1.1	4
Variation of stagnation temperature ratio in constant area duct with heat exchange (Rayleigh flow).	
1.2	5
Thermoelectric refrigerator (The Peltier effect), as quoted from Rowe (2006).	
1.3	7
Availability of increasing temperature difference across a thermoelement sides by increasing cold side temperature.	
1.4	11
General flow chart of the research methodology	
3.1	36
Typical Arrangement of Thermoelectrically Controlled Micronozzle with linear profile of TE face.	
3.2	37
Diagram of an assembly of the TECMN	
3.3	46
Micronozzle wall geometries (a) uniform TE wall, (b) non-uniform TE wall.	
3.4	51
Illustration of the quasi-one-dimensional TE model	
3.5	60
Model under test and its mesh	
3.6	61
Variable viscosity components of the propellant mixture of gases from decomposed Hydrogen-peroxide.	
3.7	66
Three different suggested profiles for $P(x)$ having same power input.	
4.1	74
Mach number versus normalized distance results for comparison of the present solution with Shapiro (1953).	
4.2	74
Mach number versus area ratio for different isothermal wall conditions.	
4.3	75
Mach number predicted along the nozzle for different cases of wall heating and cooling (depth \times throat width = $1800 \mu\text{m} \times 240\mu\text{m}$), $\text{Kn} = 0.00048$.	
4.4	79
Changes of Mach number against wall cold side temperature variation for preheating and no-preheating cases.	
Effect of decreasing Reynolds number (mass flow rate) on the	

4.5	variation of Mach number at the exit section with wall cold side temperature.	80
	Temperature gradient for different values of HRR and EGR=1.0	
4.6	Temperature distribution throughout TE for different values of HRR, and EGR=1.0.	82
4.7	Temperature gradient at TE center for different values of HRR, and EGR=1.0.	82
4.8	Temperature distribution throughout TE for different values of EGR and HRR=0.1.	83
4.9	Temperature gradient at TE center for different values of EGR and HRR=0.1.	85
4.10	Temperature distributions throughout TE for different values of aspect ratio and specified length of 1.0 mm.	86
4.11	Temperature distributions throughout TE for different values of aspect ratio and specified initial width of 0.5 mm.	88
4.12	Temperature gradients at mid distance of TE for different values of aspect ratio and specified length of 1.0 mm.	88
4.13	Temperature gradients at midpoint of TE for different values of aspect ratio and specified initial width of 0.5 mm.	89
4.14	Difference between uniform and none uniform analysis of TE for EGR=0.1 & HRR=0.1.	89
4.15	Difference between uniform and none uniform analysis of TE for EGR=10 & HRR=0.1.	91
4.16	Difference between uniform and none uniform analysis of TE for EGR=1 and different values of HRR.	91
4.17	Mach number for several grid sizes at the exit section (left) around the centre (right) near the wall.	92
5.1	Mach number contour of two selected cases of cooling and heating, Re=900.	97
5.2	Mach number contour near the wall of the expander, Re=900.	99
5.3	Density profile at the exit section of nozzle, Re=900.	100
5.4	Static pressure profile at the exit section of nozzle, Re=900.	101
5.5		102

5.6	Mach number profile at the exit section of nozzle, $Re=900$.	103
5.7	Axial-velocity profile at the exit section for several isothermal wall conditions.	103
5.8	Static temperature profile at the exit section for several isothermal wall temperatures.	104
5.9	Thrust profile at the exit section for several isothermal wall temperatures, $Re=900$.	106
5.10	Normalized thrust against various isothermal wall temperatures.	106
5.11	Inlet stagnation pressure, and exit stagnation pressure against various isothermal wall temperatures.	107
5.12	Wall temperature profile for selected cases.	110
5.13	Streamlines at the entrance of the convergent part for nozzle with extended wall and without extended wall.	114
5.14	Thrust profile at the exit section of the nozzle for selected cases of heat generation.	116
5.15	Mach number contours for different cases of heat generation within side walls.	116
5.16	Density contours for different amounts of heat generation within side uniform walls.	118
5.17	Static temperature contours for different amounts of heat generation within side uniform walls.	118
5.18	Static pressure contours for different cases of heat generation rate within uniform side walls.	119
5.19	Sound speed contours for different cases of heat generation within uniform side walls.	120
5.20	Velocity contours for different cases of heat generation within uniform side walls.	120
5.21	Specific impulse for different thermoelectric power input and through range of Reynolds numbers.	123
5.22	Specific impulse efficiency for different thermoelectric power input and through range of Reynolds numbers.	123
	Improvement of specific impulse efficiency for different	

5.23	thermoelectric power input compared with adiabatic wall.	124
5.24	Normalized thrust for different thermoelectric power input and through range of Reynolds numbers.	125
5.25	Discharge coefficient for different thermoelectric power input and through range of Reynolds numbers.	125
5.26	Maximum wall temperature measured within the side-wall for thermoelectric power input.	127
5.27	Comparison of Specific Impulse between Constant and Variable Viscosity for Low Reynolds Numbers.	129
5.28	Cell Reynolds number and density profile at the exit section for $Re=40$ and several input powers.	130

LIST OF SYMBOLS

A	Cross sectional area (m^2)
a	Initial thickness of non-uniform TE (m)
A^*	Throat area (m^2)
A_f	Area of outlet section (m^2)
A_i	Area of inlet section (m^2)
C_d	Discharge coefficient
C_p	Specific heat at constant pressure (kJ/kg.K)
C_{vo}	Exhaust velocity coefficient
D	Duct diameter (m)
d	Depth (m)
f	Friction coefficient
f_r	Friction coefficient
g_o	Gravitational acceleration (m/s^2)
h	Heat convection coefficient ($W/m^2.K$)
h_1	Enthalpy at sections 1 (J)
I	Electrical current (Amp)
I_{sp}	Specific impulse (s)
I_{sp}^{optim}	Optimum (theoretical) specific impulse (s)
J	Electric current density (Amp/m^2)
k	Thermal conductivity ($W/m.K$)
k_A	Area variation coefficient

Kn	Knudsen number
L	Length (m)
M	Mach number
\dot{m}	Mass flow rate (Kg/s)
N	Number of numerical steps
P	Perimeter (m)
P_{input}	Power input (W)
p_o	Stagnation pressure (N/m ²)
p_∞	Ambient pressure (N/m ²)
p_{exit}	Pressure at the exit section (N/m ²)
q	Heat flux (W/m ²)
Q_{cold}	Heat absorbed at the cold side (W)
Q_{hot}	Heat rejected at the hot side (W)
R	Specific gas constant (J/kg.K)
R_{cond}	Thermal conduction resistance (K/W)
R_{conv}	Thermal convection resistance (K/W)
Re	Reynolds number
S	Seebeck coefficient (V/K)
T	Temperature (K)
T_{ad}	Adiabatic wall temperature (K)
T_c	Cold side temperature (K)
T_{gas}	Gas temperature (K)
T_h	Hot side temperature (K)
T_M	Mean absolute temperature (K)
T_o	Gas stagnation temperature (K)

T_o^*	Gas stagnation temperature at throat (K)
T_w	Wall temperature (K)
V	Gas velocity (m/s)
W	Wall thickness (m)
x	Displacement in x-coordinate (m)
y	Displacement in y-coordinate (m)
Z	Figure of merit

Greek symbols

α	Aspect ratio: length per initial thickness ratio (L/w_o)
γ	Specific ratio
ΔT	Temperature difference, $T_H - T_C$ (K)
η_{nozzle}	Nozzle thermal efficiency
η_{sp}	Specific impulse efficiency
λ	Thermal conductance (W/K)
μ	Viscosity ($N.s/m^2$)
π_{ab}	Peltier coefficient (V)
ρ	Density (kg/m^3)
ρ_{elc}	Electrical resistivity ($\Omega.m$)
\Re	Recovery factor
σ	Electrical conductivity (S/m)
τ	Nozzle thrust (N/m depth)

Subscripts

I	Refers to section one
-----	-----------------------

2 Refers to section two

actu Actual

ad Adiabatic

id Ideal

LIST OF ABBREVIATIONS

2D	Two dimensional
3D	Three dimensional
AUSM+	Modified advection upwind splitting method
C.O.P.	Coefficient of performance
DSMC	Direct simulation Monte Carlo
EGR	Energy growing ratio
et al.	<i>(et alia)</i> : and others
etc	<i>(et cetera)</i> : and so forth
FEM	Finite element Method
F.D.	Fine discrete
FVM, FV	Finite Volume Method
GSFC	NASA/Goddard space flight centre
HRR	Heat resistance ratio
i.e.	that is
MEMS	Micro electro mechanical system
NS	Navier-Stock
R.K.	Runge-Kutta scheme
SPICE	Simulation program with integrated circuit emphasis
TE	Thermoelement
TECMN	Thermoelectrically controlled micronozzle
UDF	User defined function

CHAPTER ONE

INTRODUCTION

1.1 BACKGROUND

Miniaturization of engineering systems is one of the distinct characteristics of modern industry. With obvious strict limitations on weight and size, space industry is, by no means, an exception. The future of satellite technology advances toward launching increasingly smaller satellites. Small satellites may be classified according to their weight into Micro-satellites (<100 kg), Nano-satellites (<10 kg), and Pico-satellites (< 1 kg). A mission which is typically performed by one big satellite can be done by a group of Nano-satellites with a fraction of the required budget. The number of launched micro and nano-satellites increased during the last two decades, further a significant presence of nano-satellites (< 20 kg) in the past last decade, as the recent statistics given by Cheah and Chin (2011). Those trends in the spacecraft industry are driving the development of low-thrust propulsion systems. These may be needed for fine attitude control or to reduce the mass of the propulsion system through the use of small lightweight and micro scale components. However, MEMS supersonic micronozzle, a key component of micropropulsion systems, has suffered from low efficiency due to viscous effect in micro scale. Micro-scale flow analysis differs from macro-scale one in many aspects. First, the hydrodynamic slip and the thermal temperature jump conditions may arise on the micro-scale level as a consequence of the rarefied gas flow. Secondly, viscous losses are more significant at low Reynolds numbers, and viscous dissipation on a micro-scale level changes the temperature distribution because it works as an energy source, which is induced by the shear stress.

This in turn will affect heat transfer rates. Moreover, due to the reduced physical size of microthrusters, surface effects such as friction and heat transfer can dominate the gas flow in such devices, at which may require cooling. In this research, the wall temperature and wall heat fluxes play a significant role in controlling the gaseous flow and thruster performance.

1.2 THERMOELECTRICALLY CONTROLLED MICRONOZZLE

The effects of area change, friction and heat transfer on compressible flow have been separately considered in the literature. A convergent-divergent nozzle under the effect of heat adding or removing through a thermoelectric wall is configured for better expected performance. Heat exchange with the flow across the nozzle walls is one of the important effects that may have a direct impact on the properties of the flow especially when the surface area-to-volume ratio is high. Thermoelectric effect is proposed to provide heating in the convergent part and cooling in the divergent part of a micronozzle. We call such micronozzle a thermoelectrically controlled micronozzle (TECMN).

Compressible gas flow through a duct, whose cross-sectional area is varying, occurs in many engineering devices, including nozzles. The general effects of area variation on the isentropic flow through a nozzle are derived from the conservation laws, the ideal gas law, and the definition of Mach number. The physical effects of area change on Mach number (M) are summarized as stated by Shapiro (1953);

When $M < 1$ (subsonic flow), and A increases, M decreases.

When $M > 1$ (supersonic flow), and A increases, M increases.

When $M = 1$, $dA = 0$.

The results above show that if a subsonic flow is to be accelerated to a supersonic velocity it must be passed through a convergent-divergent passage or nozzle. The convergent portion accelerates the flow up to a Mach number of sonic velocity at the throat, and the divergent section then accelerates the flow to supersonic velocity. At the throat, since $dA=0$, the Mach number is sonic. The duct area at which the critical conditions (sonic velocity) exist is signed as A^* , where Mach number M^* is equal to (1) at this section.

Heat addition or removal may result, for example, from the heating or cooling of the wall of the duct through which the gas is flowing or from chemical reactions that occur in the flow such as in a combustion chamber or due to evaporation of liquid droplets being carried in the flow. The effect of heating or cooling of the flow appears in changing the stagnation temperature of the flow. The physical changes due to changing stagnation temperature of the flow are shown in the figure below, which is drawn from using the Mach number-stagnation temperature relation explained in Oosthuizen and Carscallen (1997).

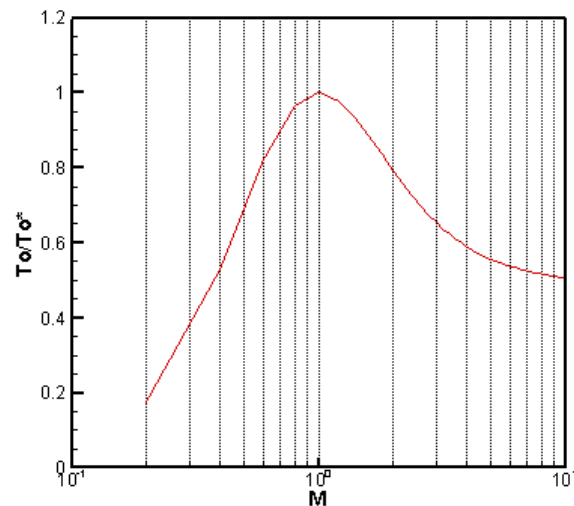


Figure 1.1: Variation of stagnation temperature ratio in constant area duct with heat exchange (Rayleigh flow).

It is evident from the Figure 1.1 that, if heat is added to the flow, the Mach number tends towards (1) while if heat is extracted from the flow, the Mach number moves away from (1) in both subsonic and supersonic flow. In other words, heating accelerates the subsonic flow and decelerates the supersonic flow, whereas cooling decelerates the subsonic flow and accelerates the supersonic flow; Figure 1.1.

1.3 THERMOELECTRICITY

Temperature gradient induces through a thermoelement (TE) supplied to an electrical field at the junctions due to the occurrence of heat pumping from the cold side to the hot side. The lateral surface of the TE is a not isothermal surface due to the temperature gradient within the TE. The temperature at the TE surface drops from hot temperature T_H to the cold temperature T_C . Typically, TE is assumed to be insulated on the lateral surfaces. So, heat exchange is normally considered and calculated at the junctions only. The TE planned to be used here is insulated at all lateral surfaces

except the side which is exposed to gas flow. As a result of Peltier effect, the rate of heat pumping at the cold junction (T_c) is given by $\pi_{ab}I$. Using the Kelvin's relationship ($S = \pi_{ab} / T_c$), we can write;

$$\pi_{ab}I = S(T_M - \Delta T / 2)I \quad (1.1)$$

Or

$$q = S(T_c) * I \quad (1.2)$$

S is the Seebeck effect coefficient ($S=V/\Delta T$) which is measured in V/K or more often in $\mu\text{V}/\text{K}$, T_M is the mean absolute temperature $(T_H+T_C)/2$ and ΔT is the temperature difference T_H-T_C as defined by Rowe (1995).

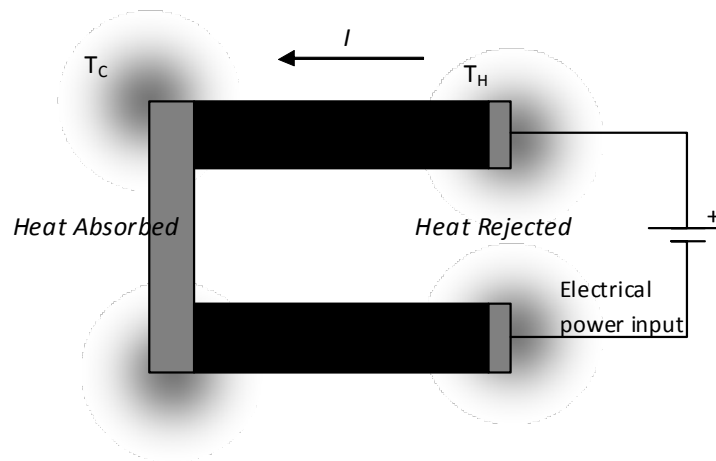


Figure 1.2: Thermoelectric refrigerator (The Peltier effect), as quoted from Rowe (2006).

The cooling effect at the source junction is opposed by Joule heating in the thermoelement (TE) and by heat conducted from the hot junction to the cold one. Half of the overall Joule heating travels to each of the junctions. Thus, the rate of absorption of heat from the source (at the cold side) is given by;